



## THE SIMULATED RESPONSE OF THE BOTTOMSIDE IONOSPHERE TO AP INDEX VARIATIONS IN MID-LATITUDES

Shun-Rong Zhang and Xin-Yu Huang

*Wuhan Institute of Physics, the Chinese Academy of Sciences, P. O. Box 71010, Wuhan 430071, P. R. China*

### ABSTRACT

Using a semi-theoretical ionospheric model for mid-latitudes, we follow the response of the bottomside electron density structure to changes in the Ap index for October 1980 and 1992. Ap values between 10 and 150 cause variations in neutral composition, temperature and winds, according to MSIS86 and HWM90 models. It is found that (1) the appearance of the F<sub>1</sub>-ledge during low solar activity becomes more pronounced with increasing Ap independent of latitude and longitude; (2) the model value foF<sub>2</sub> tends to decrease with increasing Ap. This effect is less evident at lower latitudes. Furthermore, foF<sub>2</sub> is characteristically modified by Ap in the eastern hemisphere especially for the 120-180°E sector; (3) hmF<sub>2</sub> moves up in response to Ap index enhancement. Such motions are more evident during the day and in the western hemisphere.

©1998 COSPAR. Published by Elsevier Science Ltd.

### INTRODUCTION

Variations in geomagnetic activity (described by Ap index) cause atmospheric changes in composition, temperature and horizontal winds. Such effects are modeled empirically by the MSIS86- (Hedin, 1986) and HWM90-model (Hedin *et al.*, 1991). We present results of model calculations emphasizing variations in the ionospheric ionization structure caused by geomagnetic changes. The ionospheric electron and ion density model for mid-latitudes elucidates the response of the bottomside electron density profile and characteristics to specific Ap index changes.

### THE METHOD

The time-dependent and one-dimensional ionospheric model used in this study provides the density profiles of 4 ionic species, O<sup>+</sup>, NO<sup>+</sup>, O<sub>2</sub><sup>+</sup> and N<sub>2</sub><sup>+</sup>, as well as the electron density. 21 chemical reactions for both stable and meta-stable [O<sup>+</sup>(<sup>2</sup>D) and O<sup>+</sup>(<sup>2</sup>P)] ions are involved. The molecular ion density is determined by the photochemical equilibrium assumption. O<sup>+</sup> density is obtained by solving the continuity equation and the equation of motion in the vertical direction where gravity, pressure gradient and the horizontal thermospheric wind are taken into account. The E×B drift, usually included and defined by an

empirical model for mid-latitudes in the model, is ignored for this specific study. We assume a photochemical equilibrium at 100 km as a lower boundary condition for  $O^+$ . The  $O^+$  density at upper boundary is determined generally by IRI90 (Bilitza, 1990), but when there is observational  $foF_2$  available, these IRI-based upper boundary values may also be modified so that the observed  $foF_2$  can be reasonably reproduced. For the present simulation, however, we do not introduce such modifications. We neglect also the effect of the vibrationally excited  $N_2$ . Ratios of photoelectron to EUV ionization rates given by Richards and Torr (1988) are used to calculate the photoelectron ionization. The solar irradiation fluxes are obtained from EUV91 (Tobiska, 1991), and the plasma temperatures from IRI90 which ignores an  $A_p$  index dependence. The MSIS86 and HWM90 models are applied to specify neutral composition, temperature and horizontal winds. These two empirical models provide quantitative estimations of the atmospheric changes as a function of geomagnetic activity (described by  $A_p$ ), and through which we can then introduce the  $A_p$  index effect for the present investigation. The assumption describing all variables as functions of height and time only just applies to the individual calculation related to a particular location. It does not imply the independence on latitude and longitude for the variables. Due to the above mentioned features, this model could be valid for mid-latitudes at altitudes 100-500 km. Details about the photochemical and dynamic schemes and previous results are given by Zhang and Huang (1995) and Zhang *et al.* (1996).

To investigate the  $A_p$  index control of the ionospheric structure, model calculations were carried out for a sequence of  $A_p$  values between 10 and 150 with an increment of 20. We refer to Millstone Hill (42.6°N, 288.5°E) for October 1980 and 1992 with 12-month-running sunspot medians of 150.2 and 76.4 respectively.

## RESULTS

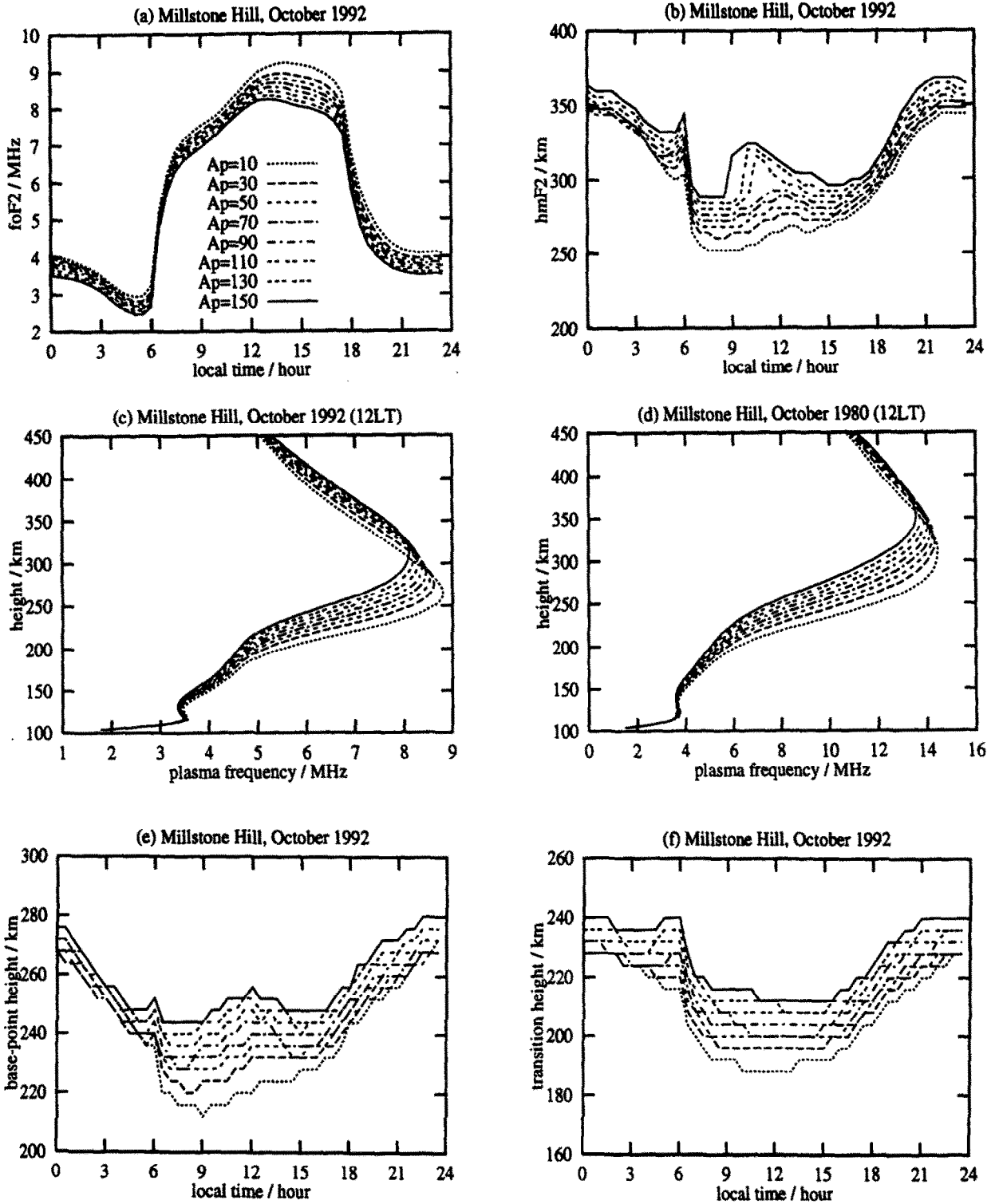
### Ionospheric Response to $A_p$ index Changes at Fixed Mid-latitude Location

Figure 1 shows the ionospheric response to  $A_p$  changes at Millstone Hill.  $foF_2$  is found to decrease with increasing  $A_p$ , while  $hmF_2$  ascends (Figures 1a, 1b). Absolute changes of these peak parameters are always larger during the day than during the night. Absolute or relative changes in  $hmF_2$  are always smaller during night. In 1980 (high solar activity), the development of the  $F_1$ -ledge, which is presently less evident, is not significantly enhanced by increasing  $A_p$  (Figure 1d). In 1992 a well-developed  $F_1$ -ledge becomes more evident (Figure 1c). Besides, the altitude of maximum electron density gradient along the vertical direction (base-point) and the lower transition height rise up with  $A_p$  (Figures 1e, 1f).

The percentage of the electron density reduction given by our simulations seems not so large as expected. That might be due to the effects which are all ignored of the vibrationally excited  $N_2$  as well as the possible dependence of the upper boundary  $O^+$  density on  $A_p$  values.

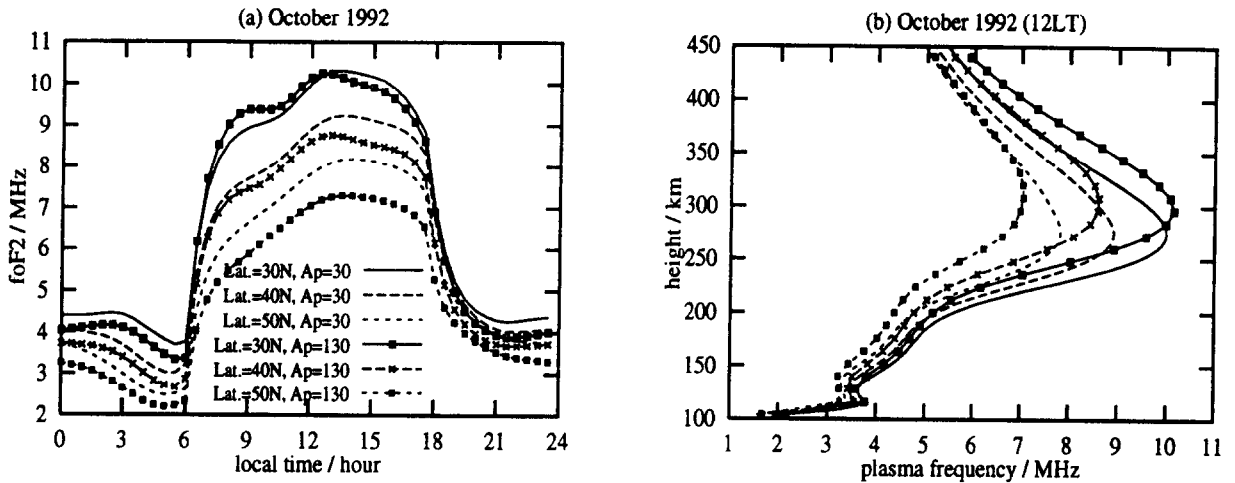
### Latitudinal Differences of the Ionospheric Response to $A_p$ Index Changes

Figure 2 displays latitudinal effects of the ionosphere due to  $A_p$  index changes. We consider two  $A_p$  values 30 and 130, and latitudes of 30°N, 40°N and 50°N. At the longitude of Millstone Hill (288.5°E), and 30°N latitude,  $foF_2$  decreases during day except for pre-noon hours. At 40°N latitude it decreases for



**Fig. 1.** Ionospheric responses to Ap Index changes at Millstone Hill (42.6°N, 288.5°E) in October. (a) foF2 for 1992 (b) hmF2 for 1992 (c) profiles at noon for 1992 (d) profiles at noon for 1980 (e) the height of base-point for 1992 (f) the lower transition height for 1992. The legend for each curve is shown in (a).

almost the whole day, and at 50°N latitude it is obviously reduced (Figure 2a).  $hmF_2$ , however, remains enhanced for all three latitudes. The  $F_1$ -ledge is slightly more evident at lower latitudes, which also applies even for dramatically increasing  $A_p$  (Figure 2b).



**Fig. 2.** Latitudinal differences of the ionospheric responses to  $A_p$  index changes, (a)  $foF_2$  for October 1992 (b) profiles at noon of October 1992. The legends are shown in (a).

### Longitudinal Differences of the Ionospheric Response to $A_p$ Index Changes

At the latitude of Millstone Hill (42.6°N), longitudinal effects are shown in Figure 3. Smaller  $foF_2$  values are observed for all longitudes when  $A_p$  changes from 30 to 130. The response of the maximum electron density is more sensitive to the  $A_p$  variation in the 120-180°E longitude sector than in other sectors (Figures 3a, 3b). The same applies to the eastern hemisphere compared to the western hemisphere. On the contrary, the  $hmF_2$  response is more sensitive in the west than in the east. The  $F_1$ -ledge, slightly more developed in the western hemisphere, becomes more evident in the west also as a result of  $A_p$  index enhancement (Figures 3c, 3d).

### CONCLUSIONS

The present investigation leads to the following primary conclusions:

- (1) The  $F_1$ -ledge appearing during low solar activity becomes more evident with increasing  $A_p$ , a situation independent on latitude and longitude;
- (2) The simulated  $foF_2$  tends to decrease with increasing  $A_p$ . This trend is less evident at lower latitudes. The electron density responds more sensitive in the eastern hemisphere especially for the 120-180 °E sector;

(3)  $hmF_2$  moves up in response to Ap index enhancement. Such a motion is more evident during the day and in the western hemisphere.

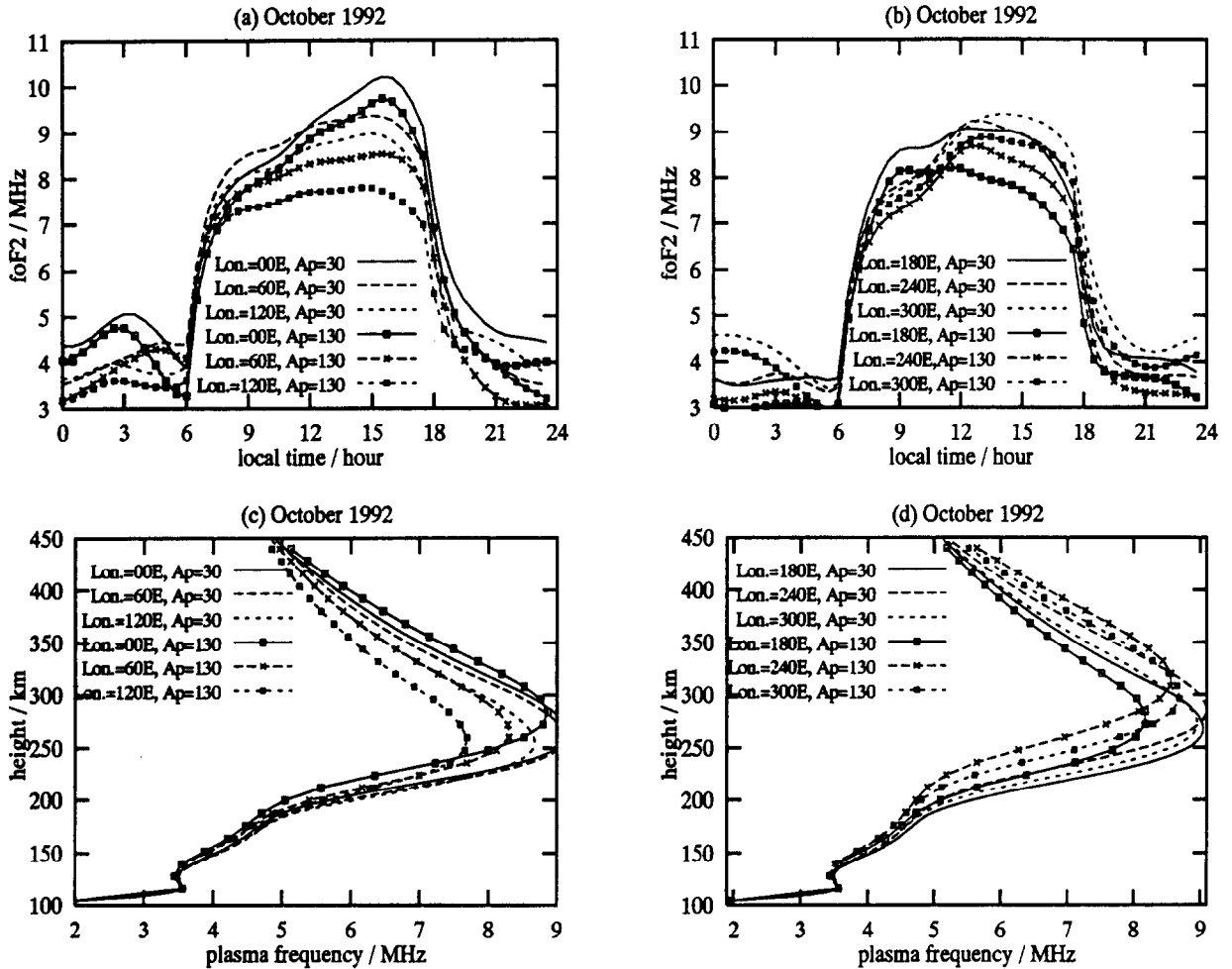


**Fig. 3.** Longitudinal differences of the ionospheric responses to Ap index changes.  
**(a)**  $foF_2$  for the eastern hemisphere **(b)**  $foF_2$  for the western hemisphere  
**(c)** profiles at noon for the eastern hemisphere **(d)** profiles at noon for western hemisphere.

**Acknowledgements:** This work was supported by the National Natural Science Foundation of China.

**REFERENCES**

Bilitza, D., International Reference Ionosphere 1990, NSSDC/WDC-A R&S 90-22, Greenbelt, Md., U.S.A. (Nov. 1990).

- Hedin, A. E., MSIS-86 thermospheric model, *J. Geophys Res.*, **92**, 4649-4662 (1987).
- Hedin, A. E., M. A. Biondi, R. G. Burnside, G. Hernandez, R. M. Johnson, *et al.*, Revised globe model of thermospheric winds using satellite and ground-based observations, *J. Geophys. Res.*, **96**, 7657-7688 (1991).
- Tobiska, K., Revised solar extreme ultraviolet flux model, *J. Atmos. Terr Phys.*, **53**, 1005-1018 (1991).
- Richards, P. G. and D. G. Torr, Ratios of photoelectron to EUV ionization rates for aeronomic studies, *J. Geophys. Res.*, **93**, 4060-4066 (1988).
- Zhang S.-R. and X.-Y. Huang, A Numerical Study of Ionospheric Profiles for Mid-Latitudes, *Ann Geophysicae*, **13**, 551-557 (1995).
- Zhang S.-R., M.-L. Zhang, S. M. Radicella, X.-Y. Huang and D. Bilitza, A comparison of the lower transition height obtained with a theoretical model and with IRI, *Adv. Space Res.*, **18**, #6, 165-173 (1996).